Ocean Dynamics (2019) 69:1053–1066
https://doi.org/10.1007/s10236-019-01289-9

Numerical modeling of the impact of hurricanes on ocean dynamics: sensitivity of the Gulf Stream response to storm's track

Tal Ezer[1]

Received: 5 September 2018 / Accepted: 11 July 2019 / Published online: 23 July 2019

Abstract
The study is focused on the disruption that a storm can cause to ocean stratification and ocean currents in a region dominated by a western boundary current and meso-scale variability. Sensitivity experiments with a regional numerical ocean model of the US East Coast are used to simulate different hurricane tracks to study the impact on the Gulf Stream (GS) flow, surrounding waters and coastal sea level. Realistic simulations of Hurricane Matthew (October 2016) using surface wind and heat flux from NOAA's operational coupled forecast system were compared with idealized artificial hurricanes with tracks located at different distances from the coast (~ 200–600 km). Despite the limitation of representing realistic wind patterns by an analytical formula, coastal storm surge near the hurricane was simulated quite well. The height of the coastal storm surge was found to be very sensitive to the location of the hurricane track relative to the coast, but the impact of the hurricane on the GS flow was found to be less sensitive to the exact hurricane track, though the maximum influence was when the hurricane track passed ~ 100 km east of the GS with winds over the GS opposing the current direction. Hurricanes that passed within hundreds of kilometers from the GS caused disruption in the GS dynamics and weakening in the downstream flow of the GS that can last for many days after the storm disappeared. This indirect impact of hurricanes on the GS can elevate sea level along long stretches of the coast. The impact of a hurricane on a region dominated by meso-scale variability is complex, creating unpredictable spatial changes in temperatures and currents. After the hurricane disappeared and without additional surface heating, it may take the stratification as much as 2 months to recover to pre-hurricane conditions by advection alone. This lasting impact of a storm on ocean dynamics is consistent with observations that show minor tidal coastal flooding that lasts for days after hurricanes passed offshore.

Keywords Coastal sea level · Hurricanes · Flooding · Gulf Stream · Florida current

1 Introduction

Tropical storms and hurricanes affect surface ocean temperatures by extracting heat from the ocean and inducing mixing that cools the upper layers along the path of the storm (Bender and Ginis 2000; Shay et al. 2000; Li et al. 2002; Oey et al. 2006, 2007; Yablonsky et al. 2015). However, the interaction between ocean currents and hurricanes can be complex, especially when hurricanes pass near western boundary currents and areas with strong meso-scale activity. For example, Oey et al. (2006) simulated the interaction of Hurricane Wilma (2005) with the Loop Current in the Gulf of Mexico, and studies of the impact of hurricanes on the Gulf Stream (GS) include Hurricane Bill in 2009 (Kourafalou et al. 2016), Hurricane Matthew in 2016 (Ezer et al. 2017; Ezer 2018b) and Hurricanes Irma Jose and Maria in 2017 (Todd et al. 2018). Other studies looked at the interaction between tropical cyclones and the Kuroshio (Wu et al. 2008; Liu and Wei 2015). These interactions can affect ocean dynamics and indirectly impact coasts farther away from the direct impact of storm surges. The motivation for the current study comes from recent findings, which showed that hurricanes and tropical storms can cause a reduction in the transport of the GS transport, and that this change can result in elevated coastal sea level and increased flooding (Ezer and Atkinson 2014, 2017; Ezer et al. 2017; Ezer 2018a, b). For example, altimeter data, cable data and high-frequency radar data (CODAR) showed

This article is part of the Topical Collection on the *10th International Workshop on Modeling the Ocean (IWMO), Santos, Brazil, 25–28 June 2018*

Responsible Editor: Huijie Xue

✉ Tal Ezer
tezer@odu.edu

[1] Center for Coastal Physical Oceanography, Old Dominion University, 4111 Monarch Way, Norfolk, VA 23508, USA

as much as 50% reduction in the GS flow after Hurricane Matthew (Ezer et al. 2017) and glider data detected as much as 40% reduction in the GS flow following Hurricanes Irma Jose and Maria (Todd et al. 2018); both studies suggested that the impact may last for a couple of weeks after the hurricanes, but they did not quantify the relation between the track of the hurricane and the impact on the GS.

The connection between coastal sea level variability and variations in the GS flow due to changes in sea level slope across the stream was suggested some time ago based on limited observations (Blaha 1984); this idea has now been confirmed by satellite data (Ezer et al. 2013) and models (Ezer 2016). In recent years, there is also renewed attention to this issue because of sea level rise—relatively small water level anomalies that were ignored in the past—can now cause tidal flooding to low-lying areas. On short time scales, the transfer of offshore large-scale signals into the coast involves barotropic open ocean waves and barotropic and baroclinic coastal trapped waves, but similar GS-coastal sea level relation was also found on interannual, decadal, and longer time-scales (Boon 2012; Sallenger et al. 2012; Ezer and Corlett 2012; Ezer et al. 2013; Ezer 2013, 2015; Goddard et al. 2015; Park and Sweet 2015; Wdowinski et al. 2016). In general, whenever the GS slows down (for a few days or on decadal time-scales), coastal sea level tends to rise above normal levels.

The source of short-term (days to annual) variability in the GS can be natural mesoscale-driven, wind and pressure-driven or seasonal variations in the subtropics that affect the flow of the Florida Current (Baringer and Larsen 2001; Meinen et al. 2010). However, the influence of tropical storms and hurricanes on the GS (Ezer et al. 2017; Ezer 2018a, b) is a new field of research that has not been fully investigated yet. In particular, recent simulations of the impact of hurricanes on the GS and the coast in a coupled model (Ezer et al. 2017) and in an ocean-only model (Ezer 2018b) focused on sensitivity to surface forcing (wind and heat flux) but left some unanswered questions: (1) the previous studies used only short simulations of 15 days, so one may wonder how long does the impact of hurricanes last? and how does the ocean recover from the impact? (2) The previous studies simulated a hurricane like Matthew with an unusual path close to the coast and close to the GS so the impact was extremely large, but one may wonder how does the track of the hurricane with respect to distance from the coast and with respect to the GS path may affect the results? Answering those questions using observations would be very difficult—in a region with active mesoscale activities and rapid changes, it is hard to separate forced response to a hurricane from natural variability. Therefore, the approach taken here was to use sensitivity experiments with an idealized hurricane and a simple ocean model of the GS and the US East Coast. The goal was not to produce the most realistic simulations but to test the sensitivity of the response to different hurricane tracks. The regional numerical ocean model is similar to that used by Ezer (2018b), but with two important modifications. First, in addition to simulations of Hurricane Matthew, experiments with artificial hurricanes tested the impact of the storm's track on the response of the GS and the coast. Second, the simulations were extended from 15 days (5 days of which had hurricane forcing) to 60 days, to allow studying the time-scale of recovery after the hurricane.

The study is organized as follows. First, the data sources and model setup are described in Sect. 2; then, the results of the different experiments are presented in Sect. 3, and finally, a summary and conclusions are offered in Sect. 4.

2 Data and model setup

The tide gauge data and the numerical model set up (Fig. 1) are the same as in Ezer (2018b), so they will be described only briefly here. The same regional numerical model was also used and described in Ezer (2016, 2017). The hourly water levels anomaly data (after removal of tides) were obtained from NOAA (http://opendap.co-ops.nos.noaa.gov/dods/). Surface heat flux and wind stress during 5 days of Hurricane Matthew (October 7–12, 2016; Ezer et al. 2017) were obtained from six-hourly output from NOAA's operational Hurricane Weather Research and Forecasting model coupled with the Princeton Ocean Model (HWRF-POM) (Yablonsky et al. 2015; Tallapragada et al. 2014); the hurricane track and maximum wind speed are shown in Fig. 2a. Note that one experiment used the HWRF-POM forcing as in Ezer (2018b), but here, the simulations were extended from 15 to 60 days and compared with 4 other simulations. The operational NOAA model was active only during the 5 days of the hurricane, so that in these sensitivity experiments, surface forcing fields (surface wind and heat flux) were set to zero outside this period—this allows to evaluate the time-scale of the recovery of the ocean after the hurricane without additional external forcing. The simulation of Hurricane Matthew by the operational HWRF coupled model has somewhat different track and intensity than that in data sets such as the Atlantic hurricane and tropical storm data HURDAT2 (Landsea and Franklin 2013; data available from NOAA's National Hurricane Center, http://www.nhc.noaa.gov/). Therefore, when constructing experiments with artificial hurricanes (see below) the HURDAT2 and HWRF data were combined to create wind field that will resemble the HWRF fields of Hurricane Matthew in the early stages (Fig. 2b). Therefore, the hurricane wind speed (W) and wind velocity components (U,V) were formulated by

$$W(x,y,t) = W_{\max}(t)\left[0.5e^{-A\Delta(x,y)/L_1} + 0.5e^{-A\Delta(x,y)/L_2}\right]$$
$$U = -W\beta\sin(\alpha); V = W\beta\cos(\alpha) \qquad (1)$$

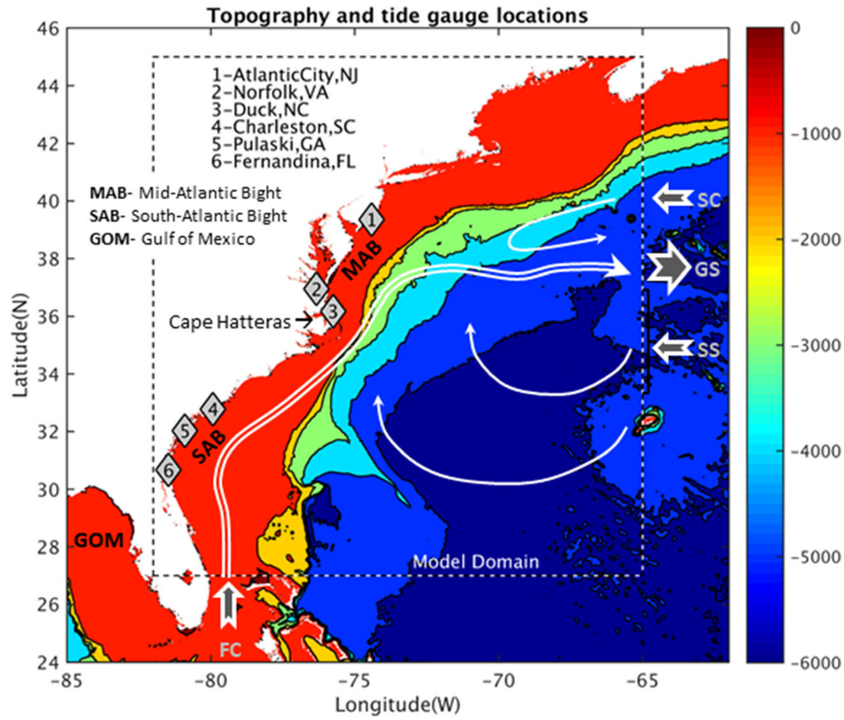

Fig. 1 Bottom topography (color in meter) of the region and model domain (dashed line). Tide gauge stations used in the study are indicated (diamonds with numbers). The location of imposed model's inflows (Florida Current, FC; Slope Current, SC and Sargasso Sea, SS) and outflow (Gulf Stream, GS) are indicated (wide arrows), as well as schematic of the main currents (narrow arrows)

where W_{max} is the maximum wind speed in m s^{-1} and Δ is the distance in km between the location of maximum speed in HURDAT2 and grid point (x,y). α is the angle from the center of the storm to the model grid point ($\alpha = 0°/180°$ for points exactly east/west of the storm) and $0.5 < \beta(\alpha) < 1$ is a factor to account for the asymmetry of the wind field (as seen in HURDAT2 data), so that winds are weaker in the back of the storm (i.e., for a northward moving storm $\beta = 1$ for $0 < \alpha < 180°$ and gradually changes to $\beta = 0.5$ for $\alpha = 270°$). Since during the last couple of days Matthew was no longer a hurricane with no data in HURDAT2, the track was artificially extended to move away from the coast and the GS. After some trial and error, the following parameters were chosen, A = 0.69, L1 = 300 km, and L2 = 600 km. The purpose was to have the artificial hurricane winds generally resemble the HWRF winds at the beginning of the simulations when the hurricane was more intense. Since the main goal here is to test the sensitivity of the impact to hurricane track, it is not crucial to exactly replicate a realistic hurricane. Nevertheless, comparison between realistic hurricane simulations and artificial ones can teach us something about the limitations of idealized hurricane representation. The result of (1) is shown in Fig. 2b. Note that when the hurricane weakened and moved offshore around October 10, the HWRF data showed a much wider area of strong winds due to interaction of the storm with other weather systems and this cannot be appropriately simulated by the artificial hurricane formula.

The model domain and lateral boundary conditions (shown in Fig. 1) are the same as in Ezer (2016, 2017, 2018b), but unlike the previous studies that focus on the impact of the GS on coastal sea level and on air-sea interactions, here the focus is on the impact of hurricane track. Following on a couple of months of spin-up, simulations of 60 days were conducted, though only 5 days (~ 6–11) include any surface forcing. Setting zero surface forcing after the hurricane dissipated has two reasons: first, HURDAT2 and HWRF-POM have no data outside the hurricane period, and second, it allows the sensitivity experiments to explore the recovery time after the hurricane without any external forcing. The horizontal grid is Cartesian with 1/12° horizontal resolution and 21 vertical sigma layers with higher resolution near the surface. Since the model has no data assimilation and no long-term realistic forcing, the GS eddies and meanders evolve from natural variability. The impact of hurricane's forcing is defined as the difference between a forced case and a control simulation without any surface forcing. Six experiments have been conducted:

1. Control case (experiment "CON," with no hurricane)—Surface heat flux and surface wind stress are zero. The only forcing is a fixed imposed boundary transports (Fig. 1): 30 Sv inflow of the Florida Current (FC), 40 Sv inflow of the Slope Current (SC), 30 Sv inflow of the Sargasso Sea (SS), and 100 Sv outflow of the Gulf Stream (GS). See Ezer (2016, 2017, 2018b) for more details on the boundary conditions.
2. Hurricane Matthew case (experiment "HM00")—Surface wind stress and heat flux were obtained from the operational coupled HWRF-POM model for October 7–12 (and zero forcing outside that period). Surface data are

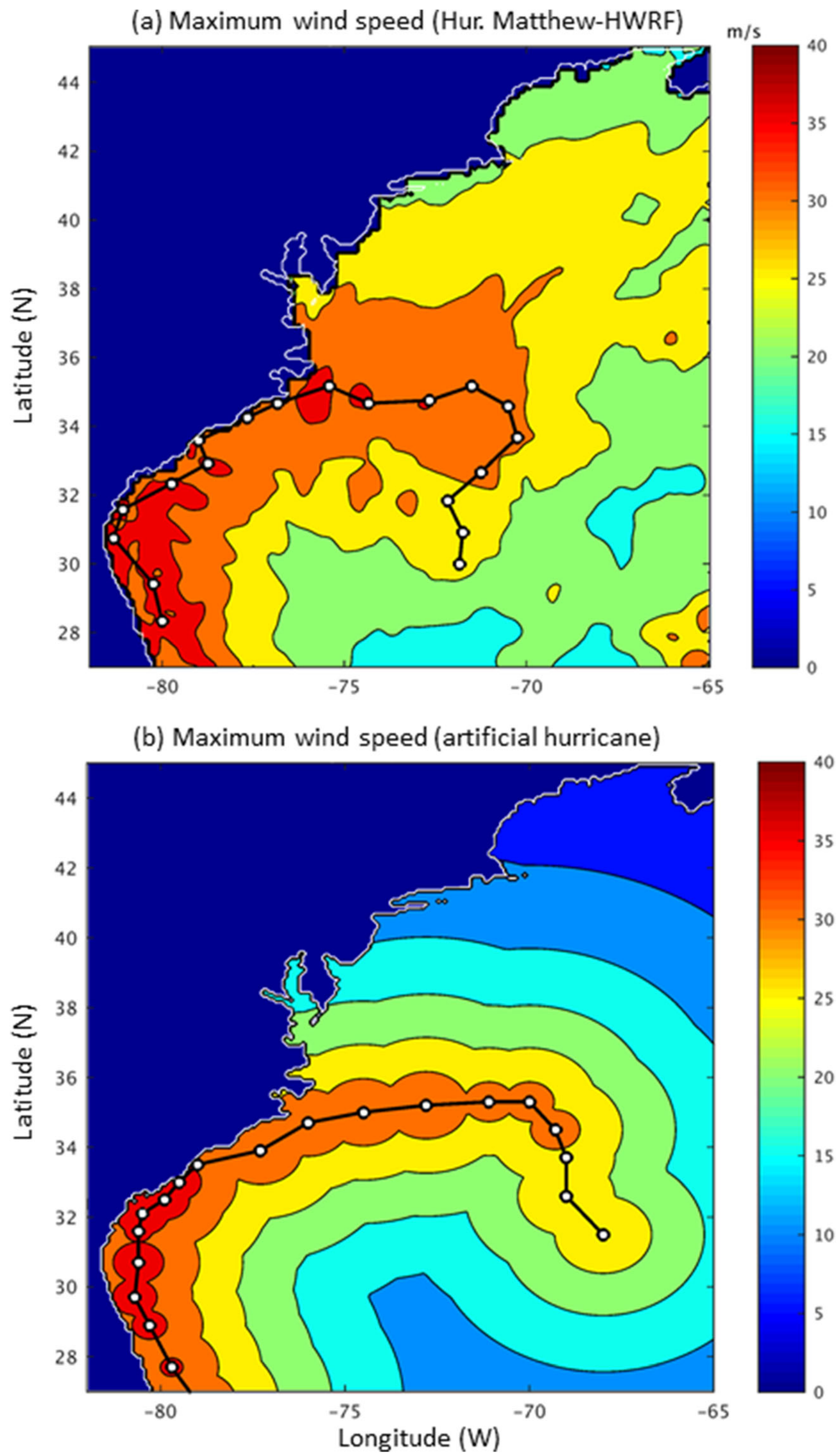

Fig. 2 The maximum wind speed (color in m s^{-1}) and track every 6 h. **a** Data from the operational forecast of the HWRF-POM coupled model for Hurricane Matthew (October 7–12, 2016; experiment HM00). **b** An artificial hurricane based on the track in HURDAT2 data and exponential decay of wind speed set to resemble Matthew (experiment AH00)

interpolated in space and time from the 6-hourly output into the ocean model grid and time. Note that unlike the coupled model in Ezer et al. (2017), here there is no feedback between the ocean and the atmosphere.

3. Artificial Hurricane following Matthew's track (experiment "AH00")—Idealized wind based on (1) was applied for 5 days. An idealized surface heat flux was derived from regression between wind speed and heat loss in HWRF (they are highly correlated near the hurricane).
4. Artificial Hurricane case (experiment "AH02")—Same as AH00, but the track was shifted by 2° eastward (away from the coast).
5. Artificial Hurricane case (experiment "AH04")—Same as AH00, but the track was shifted by 4° eastward.

6. Artificial Hurricane case (experiment "AH06")—Same as AH00, but the track was shifted by 6° eastward and 2° northward (away from the coast, but closer to the GS in the MAB).

The tracks of cases 3–6 above are shown in Fig. 3; the location of the GS in the model is also shown. The track of case 2 is shown in Fig. 2a. Note that cases 1–2 are the same experiments as in Ezer (2018b), but now they are extended from 15 to 60 days, to study the recovery time after the hurricane. Hurricane models such as HWRF (Tallapragada et al. 2014; Yablonsky et al. 2015) are continuously being tested to improve the prediction of hurricane track and intensity, and this has been a challenge for many years (Kurihara et al. 1995). These improvements are crucial for preparing for the impact of hurricane landfall. However, hurricanes that stay offshore and do not make landfall usually get less attention though their impact on the ocean and the coast can be significant, and the impact may depend on the distance of the hurricane from the coast and major ocean currents. Therefore, the tracks in Fig. 3 represent various situations, from Hurricane Matthew near the SAB coast to other cases where the hurricane is farther away from the coast. Comparisons between experiment HM00 (Hurricane Matthew track in HWRF) and experiment AH00 (artificial hurricane resembling Hurricane Matthew) will evaluate the differences between a realistic hurricane simulation and an artificial hurricane representation.

3 Results

3.1 The impact of the hurricane's track on ocean temperatures

The region of the study is one of the ocean's most active in terms of meso-scale variability, including the meandering GS and cold-core and warm-core eddies. Therefore, the impact of hurricanes on the upper ocean is complex and involves the interaction of the hurricane with the ocean. Cooling of sea surface temperature (SST) is the combination of surface heat loss due to the strong winds, vertical mixing with subsurface layers due to wind-driven ocean currents and the development of upwelling/downwelling cells. Previous simulations of Hurricane Matthew showed maximum cooling in shallow areas and on the onshore side of the GS (Ezer et al. 2017; Ezer 2018b). But what happened when the track is moved away from the coast? Figures 4, 5, and 6 show the ocean response in the experiments with artificial hurricanes with different tracks (AH00, AH02, AH04, and AH06). At the first days when the hurricane just enters the domain from the south, most of the cooling is centered around the eye of the storm, so as expected, when the track is shifted offshore, the cooling area is shifted as well (Fig. 4). However, by day 12 (Fig. 5), after the hurricane moved away from the coast and disappeared, SST in most of the model domain has cooled (by as much as ~4 °C) and there seem to be only small differences between the different experiments. In experiment AH00 (Fig. 5a) when the hurricane was closer to the coast, there was somewhat larger cooling near the

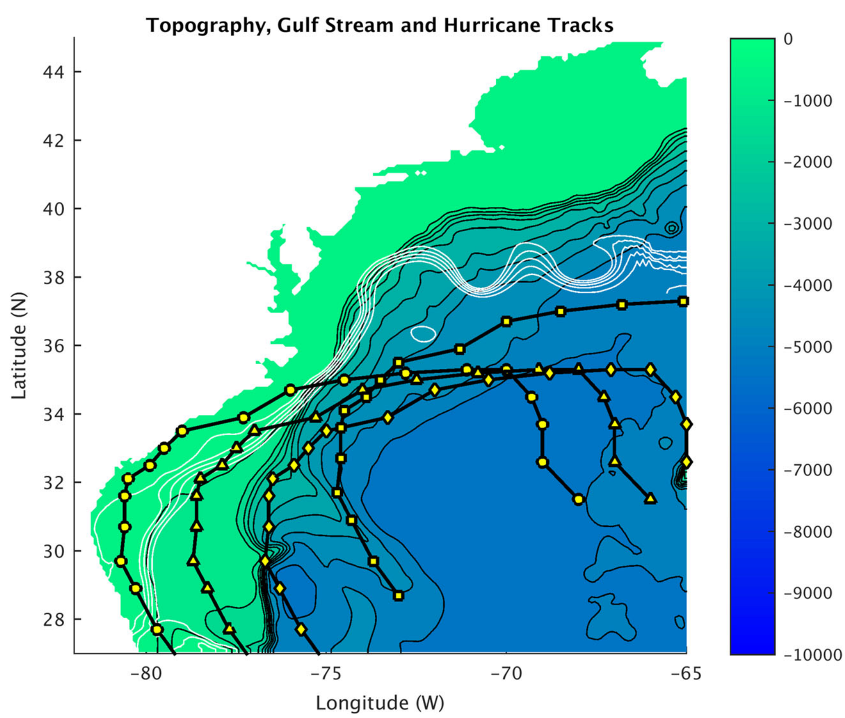

Fig. 3 Bottom depth (in meters; color and black contours) and hurricane tracks for the 4 experiments of artificial hurricane: track resembling Hurricane Matthew (experiment AH00; circles), track shifted 2 degrees east (AH02; triangles), track shifted 4 degrees east (AH04; diamonds) and track shifted 6 degrees east and 2 degrees north (AH06; squares). White contours represent the absolute sea surface height at the beginning of the experiments to indicate the location of the Gulf Stream

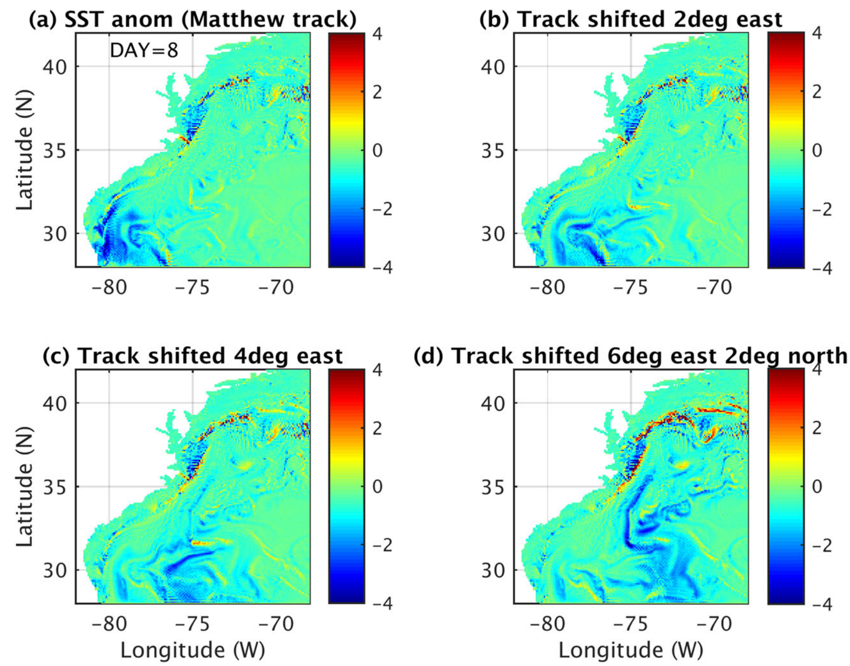

Fig. 4 Sea surface temperature change (hurricane experiment minus the control case with no hurricane) at day 8 (about second day of the hurricane) for experiments **a** AH00, **b** AH02, **c** AH04, and **d** AH06

SAB coast, and in experiment AH06 (Fig. 5d), there is somewhat larger cooling in the MAB south of the GS, but the differences are not that significant. Due to the mesoscale activities and strong currents in the region, one cannot see here the typical cooling path along the track of the hurricane as found in other cases (Bender and Ginis 2000; Oey et al. 2007). Some relative warming (relative to the no hurricane control case CON) is found on the northern edge of the GS—it appears that the change was caused when the GS and eddy fronts were eroded and shifted (Ezer 2018b). It is interesting to note of another hurricane-current interaction that resulted in unusual local warming—when Hurricane Wilma in 2005 passed near the Loop Current in the Gulf of Mexico (Oey et al. 2006). On day 30 (Fig. 6), more than 2 weeks after the hurricane disappeared, there is very little difference between the cases. Advection by the GS of warmer waters from the south had reached the MAB by that time, returning temperatures to pre-hurricane conditions. However, away from the GS, the water remained slightly

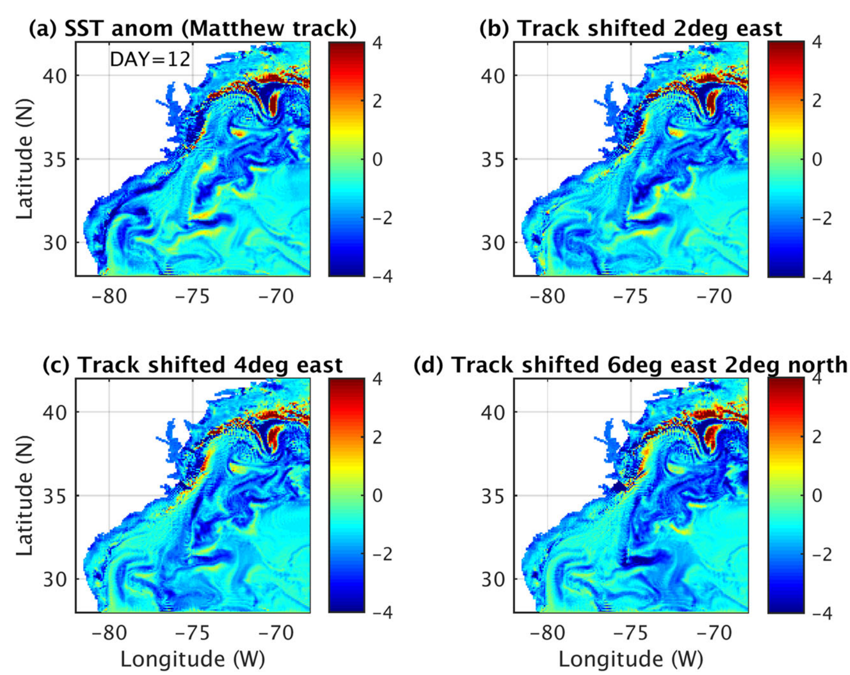

Fig. 5 Same as Fig. 4, but for day 12, after the hurricane disappeared

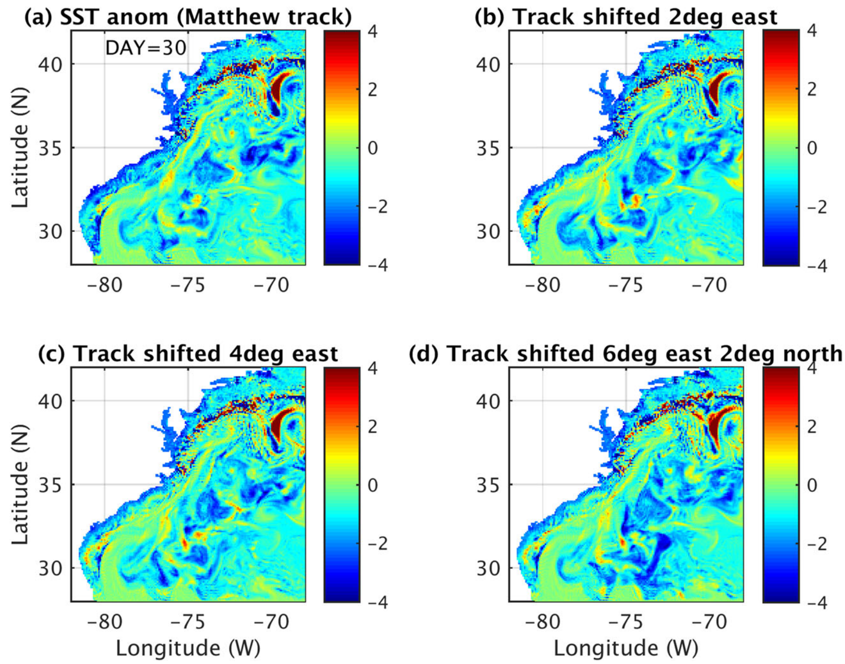

Fig. 6 Same as Fig. 4, but for day 30, about 19 days after the hurricane disappeared

colder than normal with strong spatial variations due to meso-scale eddy activity. In the real ocean, air-sea heat exchange and weather events unrelated to the hurricane would affect the temperatures during this period, but in these idealized simulations, only the advective component is considered in the recovery period. Direct comparison between the surface cooling in the idealized experiments and SST data is not possible (one does not know what the temperature would have been in the real ocean without the hurricane). However, qualitative look at satellite SST anomaly (not shown, but see NOAA data at: https://www.ospo.noaa.gov/Products/ocean/index.html) reveal about 4 °C difference at some locations between SST anomaly before and after the hurricane with spatial variations resembling the model results.

An example of the impact of the hurricane on temperatures below the surface is shown in Fig. 7 (comparing experiments AH00 and AH06 at one location in the middle of the domain; other locations demonstrate similar patterns). Again, the response is dominated by meso-scale activities and is not affected that much by the exact track of the hurricane. Only during days 10–12 the cooling and mixing of the upper 50–100 m is the direct response to the hurricane (when it was close to this site). However, with the idealized experiments of no surface heat flux or wind after the hurricane moved away, advection by the GS and eddies is the main source of temperature changes. Colder than normal waters remained in the area until days 30–40 and then during days 40–60 meso-scale activities bring cold and warm waters to this location, creating large and unpredictable spatial variations, as seen also in Figs. 4, 5, and 6.

3.2 The impact of the hurricane on coastal sea level

Observed coastal sea levels at the 6 tide gauge stations (see the locations in Fig. 1) are compared with the model simulations in Fig. 8. Only experiments HM00 and AH00 are expected to resemble the observations, and they do simulate quite well the storm surge in the SAB, especially in Fernandina, Florida (~ 2 m water level change within 1 day). However, when the hurricane moved northward alone the coast, the skill of the artificial hurricane degraded so the storm surge in AH00 is underestimated for Pulaski and Charleston. This result demonstrates the difficulty of representing the wind pattern of a storm by analytical expression with constant length-scales (L_1 and L_2 in Eq. (1)) which cannot capture the wide scale influence of a weak storm at its latest stages when it is no longer a hurricane with a distinct tight wind pattern (Fig. 2). The results are consistent with other studies which showed that storm surge forecasts based on HURDAT2 data have less skill than forecasts using hurricane data from numerical atmospheric models (Garzon et al. 2017). Far from the hurricane, in the MAB, the elevated coastal sea level was similar in HM00 and AH00, and as will be shown later, this may indicate an indirect impact from the GS rather than storm surge. When the hurricane track shifted about 200 km away from the coast (AH02), the storm surge in the SAB declined to about 30% of the observed one. However, the impact farther north in Norfolk remained similar in AH00 and AH02, which may indicate again the indirect impact by the GS, as seen before (Ezer 2016; Ezer and Atkinson 2017; Ezer et al. 2017). The case when the hurricane track was shifted farther away from the coast and farther north (AH06) caused early elevated sea level

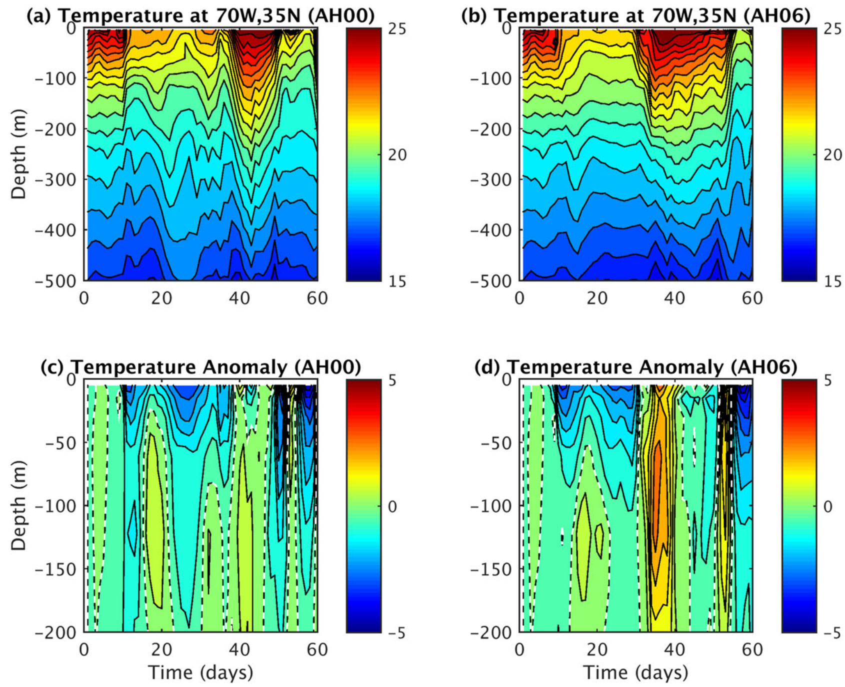

Fig. 7 Temperature change as a function of depth and time at (70° W, 35° N) for experiment AH00 (left panels) and AH06 (right panels). The top panels are the actual temperature and the bottom panels are the anomalies relative to the control experiment without a hurricane; note the change in axis and color scale. Contour intervals are 0.5 °C in **a** and **b** and 0.25 °C in **c** and **d** (dash line represents zero)

at Duck and Norfolk, even when the hurricane was some 300–600 km away from the coast.

While Fig. 8 shows the coastal sea level at selected spots, to look at the impact along the entire coast, a Hovmöller diagram of sea level anomaly as a function of time and latitude along the coast is presented in Fig. 9. For the case of Hurricane Matthew track (AH00; Fig. 9a), the hurricane propagated northward along the coast of the SAB until day 9, raising sea level (red) ahead of the storm where waters are pushed onshore and immediately lowering sea level (blue) at the wake of the storm where the winds are moving water away from the coast. Later, at days 9–12, sea level in the MAB was raised and the elevated water then propagated back to the SAB. Sea level remained elevated until day 13 in the SAB and at least until day 16 in the MAB. When the track shifted away from the coast (Fig. 9b–d), coastal sea level remained elevated almost everywhere, with no significant decline in the wake of the storm. It is interesting to note the differences between the SAB, where the hurricane track strongly influenced the storm surge and coastal sea level, and the MAB, where the track location made little impact on the coast. Note also the southward propagation of coastal trapped waves (as expected in the Northern Hemisphere, see Ezer 2016) and the clear distinction between the impact on the SAB and MAB. The sharp change in the topography at Cape Hatteras and the proximity of the coast to the GS in the SAB result in significant differences in coastal sea level variability between the MAB and SAB, as indicated in a recent study focused on spatial variations along the US East coast (Ezer 2019).

3.3 The lasting impact of the hurricane on the Gulf Stream strength and stratification

Several recent studies indicated the temporal disruption that a hurricane can cause to the GS and the consequence for elevated coastal sea level (Ezer and Atkinson 2014, 2017; Ezer et al. 2017; Ezer 2018a, b; Todd et al. 2018). However, in those studies, it was not clear how close to the GS the hurricane track should be to have an impact, and how long does the impact lasts. A measure of the strength of the GS was derived in the following way. First, from each hourly model sea level data $\eta(x,y,t)$, and for each experiment, the GS path was found by searching for maximum sea level slope (i.e., maximum surface geostrophic flow); fronts and eddies located away from the mean GS path were filtered out. Then, the slope values were normalized to represent the sea level height change in cm over 100 km distance and averaged over all points in the MAB (north of latitude 35° N). Finally, the results from the case with no hurricane were subtracted from cases 2–6 to separate the impact of the hurricane from time-dependent meso-scale variations. This procedure is like that used in Ezer et al. (2013), who looked at decadal variations in the strength of the GS. The results for the 5 experiments are shown in Fig. 10. The long-term mean slope in this region is ~ 100 cm per 100 km, so a value of − 10 cm indicates about 10% reduction in the mean surface flow of the GS relative to the same period without a hurricane. Note that at some locations and times the changes are much larger, but this is the mean change along ~ 1000 km of GS between 65° W and 75° W. In all the experiments, the GS remained weaker than normal (negative values in Fig. 10) for almost a

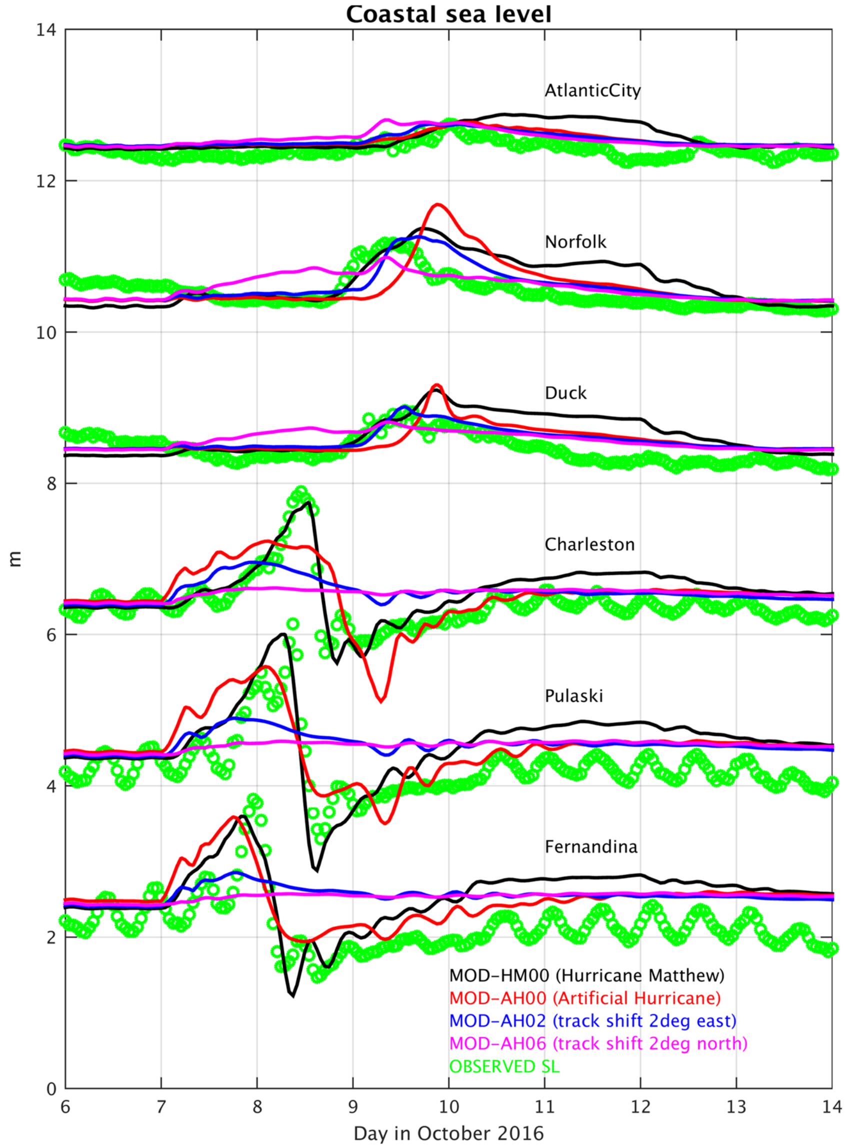

Fig. 8 Hourly coastal sea level at the locations shown in Fig. 1. Tide gauge data (anomaly relative to tidal prediction; green circles) is compared with model simulations- HM00 (black), AH00 (red), AH02 (blue), and AH06 (magenta). For clarity, mean water levels have been shifted vertically for each location

month, and the pattern of the variability was similar in most experiments despite the large changes in tracks (Fig. 3). After about day 25, the experiments separated from each other due to the nonlinear nature of the meso-scale variability, so for example, experiments HM00 (black line) and AH00 (red line) with similar tracks had opposite sign of the response by day 30. During the short period that the hurricane was active, the amplitude of the GS weakening response increased as the tracks moved away from the coast and farther east when the winds on the left side of the hurricane were in opposite direction to the GS flow. The impact of the track location relative to the GS is summarized in Fig. 11, where the mean east-west distance between the hurricane and the GS in the SAB is compared with the mean reduction in the GS strength downstream in the MAB during the 2 weeks after the hurricane entered the region (and before mesoscale activities became dominant). The maximum reduction in the GS strength was obtained in AH02, when the track was in average ~ 100 km east of the GS, so given the size of the hurricane (Fig. 2b), strong southward winds on the west side of the hurricane were close to the northward flowing GS. The difference between HM00 and AH00 (in both cases the hurricane was in average west of the GS) reflects the fact that the artificial hurricane had more compressed strong winds near the center of the storm compared with the wider wind pattern in HWRF (Fig. 2). However, in general, the differences between the experiments were not that large (~ 20–40%), so it seems that it is not necessary for a hurricane to pass exactly over the GS to have an impact, and as long as a hurricane stays for several days within 100 s of km from the GS, it can impact the dynamics. This was the case for example of Hurricane Joaquin (2015) which stayed farther offshore but had significant impact on the GS and the coast (Ezer and Atkinson 2017; Ezer 2018a).

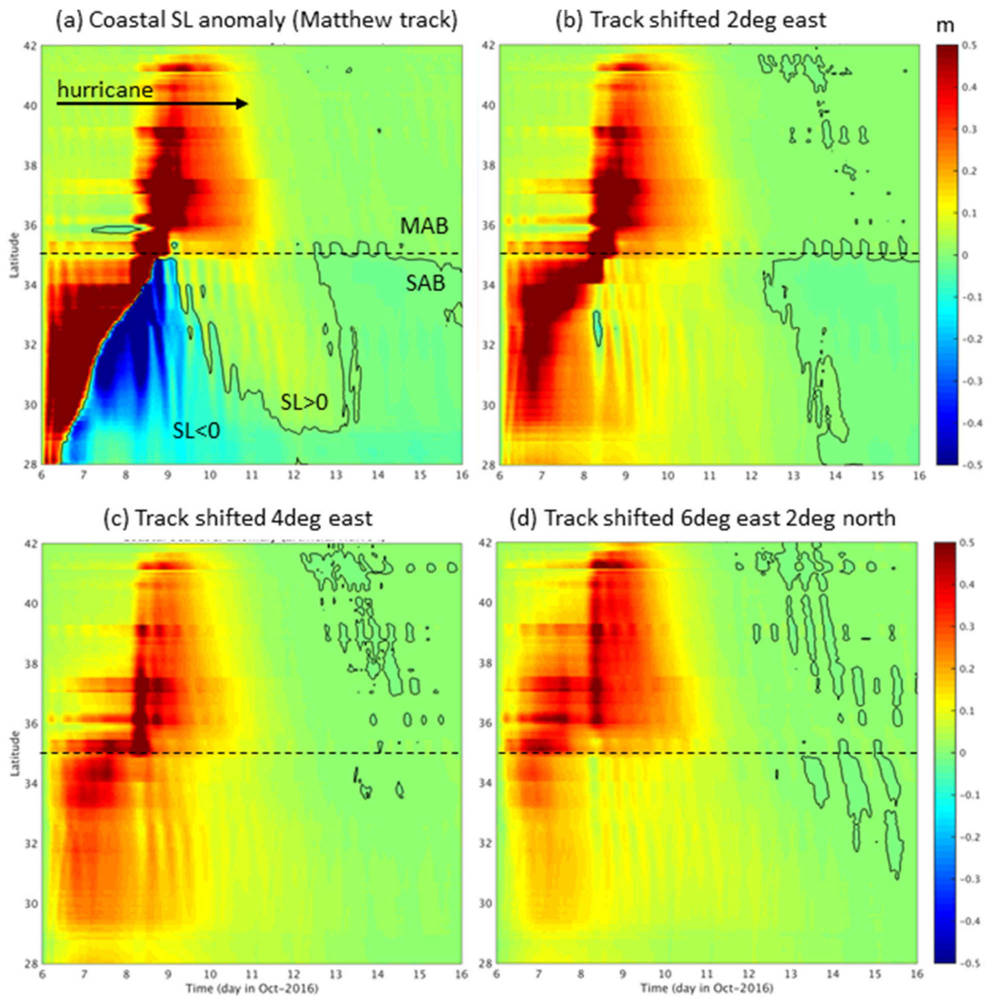

Fig. 9 Hovmöller diagram of sea level anomaly along the coast as a function of time and latitude for experiments (a) AH00, AH02, AH04, and AH06. Black contour indicates the zero line and the horizontal dash line separates between the coasts of the MAB and SAB

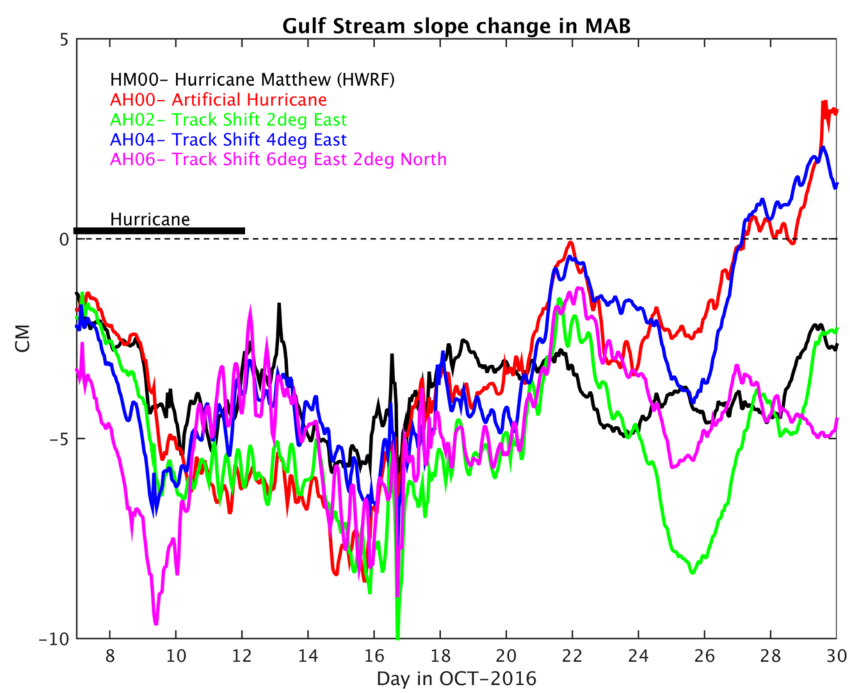

Fig. 10 The mean change in the strength of the Gulf Stream for the different experiments (relative to the control case without a hurricane), averaged over the area north of 35° N (the MAB). Shown is the change in the sea level height difference across the Gulf Stream, normalized to represent the slope over 100 km horizontal distance; the mean slope in all cases is ~ 1 m per 100 km

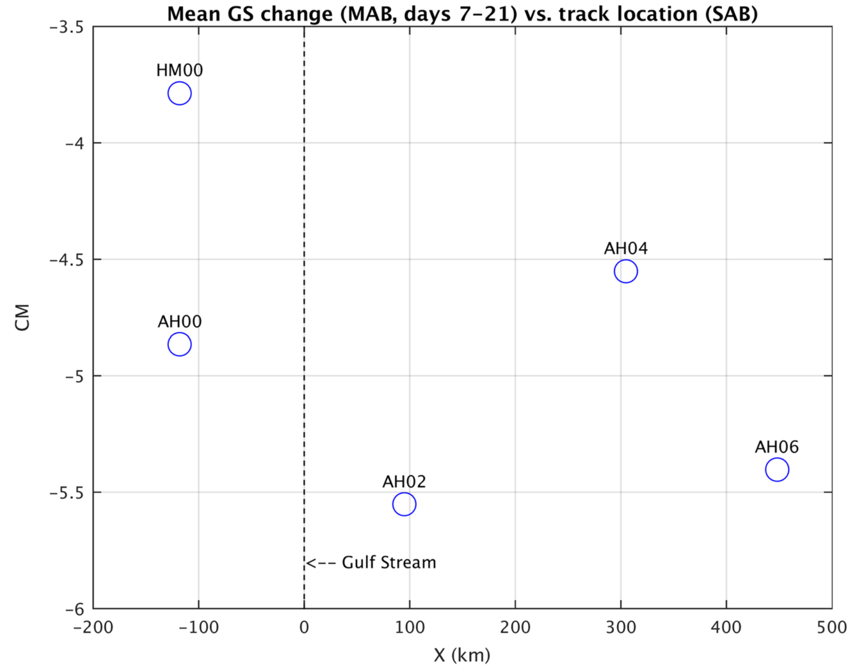

Fig. 11 The time and area mean GS strength reduction (in cm difference across the GS as in Fig. 10) over 2 weeks (October 7–21) versus the mean east-west location of the hurricane track relative to the GS location in the SAB

The lasting impact of the hurricane can be seen in the volume averaged (over all the model domain and the upper 50 m) mean kinetic energy (MKE) and mean potential energy (MPE) as shown in Fig. 12. These calculations represent the changes in velocity and stratification (negative MPE means more mixing and less stratified ocean) relative to the case with no hurricane; see Ezer (2018b) for details on these calculations over a shorter period. The spike in MKE is large and short-lived during the peak of the hurricane (around day 9), though despite the local weakening of the GS (Fig. 10), the wind-driven surface currents in the interior of the domain continue for another week or so after the wind is set to zero. The evolution of MPE is very different than MKE; it declined quickly during the hurricane, but remained negative in all the experiments for at least 60 days. The latter indicates that after cooling and mixing of the upper layers during the hurricane it takes the ocean a long time to recover. Note, however, that in these idealized experiments, surface wind and heat flux were zero outside the 5-day period of the hurricane, so the recovery involved mostly advection of new warmer waters by the GS

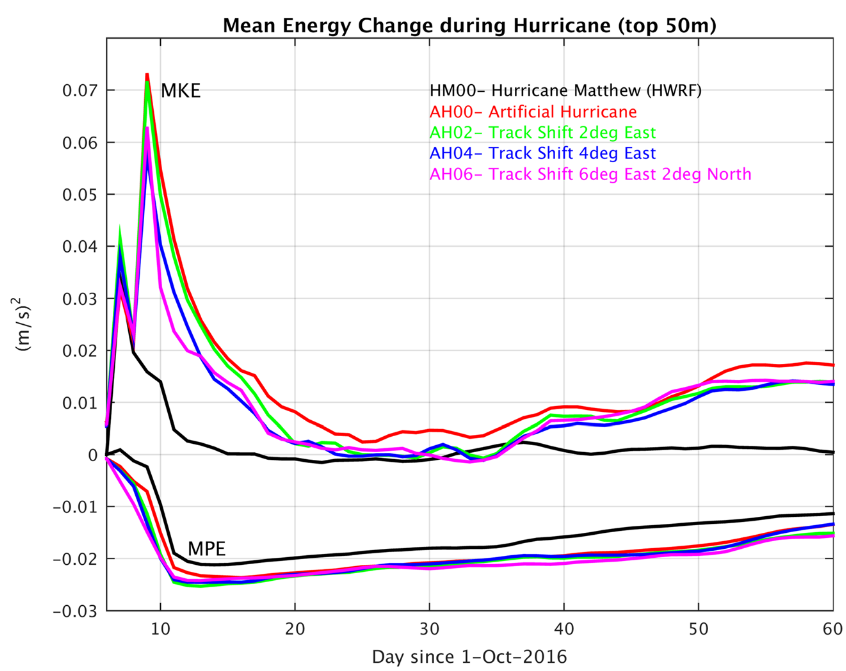

Fig. 12 Daily changes in the average mean kinetic energy (MKE, upper lines) and mean potential energy (MPE, lower lines) for the different experiments. The changes are the anomalies relative to the control run (no hurricane case). The values are energy per unit mass averaged over the upper 50 m of the entire model domain

(Fig. 6). In the real ocean, solar radiation and air-sea heat exchange can help to rebuild the stratification (or other weather systems can work to degrade it). The exact hurricane track does not seem to affect the energy change that much though all the cases with artificial hurricanes had larger change in MKE and MPE during the hurricane than the case forced with fluxes from HWRF. The artificial hurricane winds were somewhat more intense and more concentrated near the eye of the storm in comparison to the HM00 case, which could create larger MKE and stronger decline in MPE. It is not completely clear why MKE started to increase at the same rate during the last 30 days for the artificial hurricanes (all color lines except black in Fig. 12) despite their different GS flow (Fig. 10). It is possible that the location of the storm farther east in the cases of artificial hurricanes affected the flow near the eastern boundary. In this meso-scale active region, natural variations and nonlinear processes dominate so one cannot predict the behavior over long period.

4 Summary and conclusions

The role of ocean dynamics in connecting large-scale long-term climatic changes and variability with variations in coastal sea level is increasingly evident; for example, in the context of sea level rise acceleration due to potential GS or AMOC slows down (Sallenger et al. 2012; Ezer et al. 2013; Goddard et al. 2015; Park and Sweet 2015). However, ocean dynamics can also impact high-frequency coastal sea level variability that can cause short-term minor tidal flooding (Ezer and Atkinson 2014). These short-term variations can be related to natural variations in the GS flow (Meinen et al. 2010; Ezer 2016), weather systems (Li et al. 2002), variations in air pressure (Piecuch and Ponte 2015; Piecuch et al. 2016), etc. The current study focused on short-term variations due to the passage of hurricanes and their indirect impact on ocean dynamics. The study followed on the footsteps of recent studies on the impact of Hurricane Matthew (Ezer et al. 2017; Ezer 2018b). While the previous studies focused on the strong impact that the hurricane had on the coast and on weakening the GS, it was not clear if this impact was just a coincidence because of the unusual track of that hurricane or a more general response to hurricanes that move along the coast without making a landfall. The track of Hurricane Matthew followed very closely both, the path of the GS in the SAB and along the southeastern US coast—the result was flooding of many cities in Florida, Georgia, South Carolina, North Carolina, and Virginia due to the combination of storm surge and massive precipitation. Matthew, together with other tropical storms preceding it, may have caused also as much as 50% reduction in the GS flow over a few weeks that caused flooding in the MAB away from the storm (Ezer et al. 2017); the high water level due to the weaker GS exacerbate the flood damage as it prevented flooded streets from draining after the heavy rain. Following on Ezer et al.'s (2017) findings of the impact of hurricane Matthew on the GS in 2016, Todd et al. (2018) using glider data found similar reduction in the GS flow (up to 40%) following 3 hurricanes in 2017. Because the intensity and track of each real hurricane is different, it is difficult to study the impact of the track separate from other parameters with real data, so the main goal here was to systematically study the impact of the hurricane track using idealized sensitivity experiments with a numerical model.

The method to evaluate the impact of hurricane tracks was to conduct sensitivity experiments with artificial hurricanes that resemble Matthew in wind and heat flux, but with different tracks. First, it was found that representing a real hurricane with analytical expression is quite difficult because using hurricane track, size and wind speed is insufficient to represent the interaction of a hurricane with the surrounding atmospheric pattern; representing the structure of a storm after it dissipated from a tight hurricane into a weaker large weather system is especially difficult (Fig. 2). With the meandering GS and the existing of warm- and cold-core eddies, the study area is one of the most active regions in terms of meso-scale variability. Therefore, the pattern of cooling of SST in the wake of the hurricane is much more chaotic and unpredictable (e.g., Fig. 5) compared with a typical impact along the path of the hurricane (e.g., Bender and Ginis 2000). Another difficulty in assessing the impact of hurricanes in this region is that comparing conditions before and after a hurricane will result in large changes due to the meso-scale variability, so how one separates the meso-scale variability from the hurricane-induced changes? The solution here was to compare the hurricane's simulations with a control run without a hurricane. It should also be noted that the experiments here neglected the feedback between the ocean and the atmosphere, which is important for a coupled model such as HWRF-POM (Tallapragada et al. 2014; Yablonsky et al. 2015). Therefore, the experiments were meant to test the sensitivity of the response to hurricane's track, but not to reproduce the most realistic ocean simulations.

When compared with tide gauge data, it was shown that coastal storm surge near the hurricane can be simulated quite well even by the artificial hurricane with the right track and intensity, but far fields may not be simulated that well. If the hurricane track is artificially moved away from the coast, the storm surge declined as expected. However, it was found that the indirect impact of the storm on the coast through changes in the ocean dynamics was not very sensitive to the hurricane track. Whenever the hurricane passed within hundreds of miles of the GS, it had similar effects of cooling the warm waters south of the GS, disrupting the flow and diminishing the temperature gradients across the GS (Ezer 2018b). In all cases, the sea level slope across the GS, which represents the geostrophic surface flow, remained lower than normal for at least few weeks after the hurricane disappeared; the strongest impact on the GS strength was when the hurricane was ~ 100 km east of the GS, so winds were blowing against the GS flow. Potential energy, representing the stratification of the upper ocean, remained lower than pre-hurricane conditions for at least 60 days. In these idealized cases, the recovery of the GS structure was only due to advection of new warm waters from the south which reached the MAB area during this time. Air-sea exchange was neglected here, but nevertheless, the experiments demonstrated the lasting effect of the hurricane on ocean dynamics. The results of the model experiments can explain observations of minor tidal flooding that are often seen in the days after hurricanes passed offshore in the south-western North Atlantic. One such example is Hurricane Joaquin in 2015, which stayed way offshore for days without ever getting close to the coast (its track was somewhat like experiment AH06), but its impact was felt through a significant weakening of the GS that caused several days of flooding along the U.S. East Coast (Ezer and Atkinson 2017; Ezer 2018a). Another case of an offshore hurricane with large influence was Hurricane Sandy in 2012, which caused large elevated water levels and flooding along the southeastern US coast (McCallum et al. 2013) in the days before it made landfall and was still moving north ~ 500 km away from the coast. In summary, while most of the results presented here are consistent with previous studies, new findings about the impact of hurricane tracks and about the long-lasting impact of hurricanes on the GS and ocean stratification may have significant implications for improving storm surge models and predicting future sea level variability and flood risks.

Acknowledgments Old Dominion University's Climate Change and Sea Level Rise Initiative (CCSLRI) and the Resilience Collaborative (ODU-RC) provided partial support for this study, and the Center for Coastal Physical Oceanography (CCPO) provided computational support. Bob Tuleya is thanked for discussions about hurricane models. The hourly tide gauges sea level data are available from: (http://opendap.co-ops.nos.noaa.gov/dods/). The HWRF model results are available from NOAA/NCEP (http://www.emc.ncep.noaa.gov/gc_wmb/vxt/HWRF/), and some model results were provided by the hurricane group at URI.

References

Baringer MO, Larsen JC (2001) Sixteen years of Florida current transport at 27°N. Geophys Res Lett 28(16):3,179–3,182. https://doi.org/10.1029/2001GL013246

Bender MA, Ginis I (2000) Real-case simulations of hurricane–ocean interaction using a high-resolution coupled model: effects on hurricane intensity. Mon Weather Rev 128:917–946. https://doi.org/10.1175/1520-0493(2000)128<0917:RCSOHO>2.0.CO;2

Blaha JP (1984) Fluctuations of monthly sea level as related to the intensity of the Gulf Stream from Key West to Norfolk. J Geophys Res Oceans 89(C5):8033–8042. https://doi.org/10.1029/JC089iC05p08033

Boon JD (2012) Evidence of sea level acceleration at U.S. and Canadian tide stations, Atlantic coast, North America. J Coast Res 28(6):1437–1445. https://doi.org/10.2112/JCOASTRES-D-12-00102.1

Ezer T (2013) Sea level rise, spatially uneven and temporally unsteady: why the U.S. East Coast, the global tide gauge record, and the global altimeter data show different trends. Geophys Res Lett 40:5439–5444. https://doi.org/10.1002/2013GL057952

Ezer T (2015) Detecting changes in the transport of the Gulf Stream and the Atlantic overturning circulation from coastal sea level data: the extreme decline in 2009-2010 and estimated variations for 1935-2012. Glob Planet Chang 129:23–36. https://doi.org/10.1016/j.gloplacha.2015.03.002

Ezer T (2016) Can the Gulf Stream induce coherent short-term fluctuations in sea level along the U.S. East Coast?: a modeling study. Ocean Dyn 66(2):207–220. https://doi.org/10.1007/s10236-016-0928-0

Ezer T (2017) A modeling study of the role that bottom topography plays in Gulf Stream dynamics and in influencing the tilt of mean sea level along the U.S. East Coast, Ocean Dynamics 67(5):651–664. https://doi.org/10.1007/s10236-017-1052-5

Ezer, T (2018a) The increased risk of flooding in Hampton roads: on the roles of sea level rise, storm surges, hurricanes and the Gulf Stream. In: The Hampton Roads Sea Level Rise Preparedness and Resilience Intergovernmental Pilot Project, Toll, R. and G. F. Kuska (Eds.). Mar Technol Soc J 52(2):34–44, https://doi.org/10.4031/MTSJ.52.2.6

Ezer T (2018b) On the interaction between a hurricane, the Gulf Stream and coastal sea level. Ocean Dyn 68:1259–1272. https://doi.org/10.1007/s10236-018-1193-1

Ezer T (2019) Regional differences in sea level rise between the Mid-Atlantic Bight and the South Atlantic Bight: is the Gulf Stream to blame? Earth's Future. https://doi.org/10.1029/2019EF001174

Ezer T, Atkinson LP (2014) Accelerated flooding along the U.S. East Coast: on the impact of sea-level rise, tides, storms, the Gulf Stream, and the North Atlantic Oscillations. Earth's Future 2(8):362–382. https://doi.org/10.1002/2014EF000252

Ezer T, Atkinson LP (2017) On the predictability of high water level along the U.S. East Coast: can the Florida Current measurement be an indicator for flooding caused by remote forcing? Ocean Dyn 67(6):751–766. https://doi.org/10.1007/s10236-017-1057-0

Ezer T, Corlett WB (2012) Is sea level rise accelerating in the Chesapeake Bay? A demonstration of a novel new approach for analyzing sea level data. Geophys Res Lett 39:L19605. https://doi.org/10.1029/2012GL053435

Ezer T, Atkinson LP, Corlett WB, Blanco JL (2013) Gulf Stream's induced sea level rise and variability along the U.S. mid-Atlantic coast. J Geophys Res Oceans 118:685–697. https://doi.org/10.1002/jgrc.20091

Ezer T, Atkinson LP, Tuleya R (2017) Observations and operational model simulations reveal the impact of Hurricane Matthew (2016) on the Gulf Stream and coastal sea level. Dyn Atmos Oceans 80:124–138. https://doi.org/10.1016/j.dynatmoce.2017.10.006

Garzon JL, Ferreira CM, Padilla-Hernandez R (2017) Evaluation of weather forecast system for storm surge modeling in the Chesapeake Bay. Ocean Dyn 68(1):91–107. https://doi.org/10.1007/s10236-017-1120-x

Goddard PB, Yin J, Griffies SM, Zhang S (2015) An extreme event of sea-level rise along the northeast coast of North America in 2009–2010. Nat Commun 6:6345. https://doi.org/10.1038/ncomms7346

Kourafalou VH, Androulidakis YS, Halliwell GR, Kang HS, Mehari MM, Le Hénaff M, Atlas R, Lumpkin R (2016) North Atlantic Ocean OSSE system development: nature run evaluation and application to hurricane interaction with the Gulf Stream. Prog Oceanogr 148:1–25. https://doi.org/10.1016/j.pocean.2016.09.001

Kurihara Y, Bender MA, Tuleya RE, Ross RJ (1995) Improvements in the GFDL hurricane prediction system. Mon Weather Rev 123(9):2791–2801

Landsea CW, Franklin JL (2013) Atlantic hurricane database uncertainty and presentation of a new database format. Mon Weather Rev 141: 3576–3592

Li Y, Xue H, Bane JM (2002) Air-sea interactions during the passage of a winter storm over the Gulf Stream: a three-dimensional coupled atmosphere-ocean model study. J Geophys Res Oceans 107(C11). https://doi.org/10.1029/2001JC001161

Liu X, Wei J (2015) Understanding surface and subsurface temperature changes induced by tropical cyclones in the Kuroshio. Ocean Dyn 65(7):1017–1027. https://doi.org/10.1007/s10236-015-0851-9

McCallum BE, Wicklein SM, Reiser RG, Busciolano R, Morrison J, Verdi RJ, Painter JA, Frantz ER, Gotvald AJ (2013) Monitoring storm tide and flooding from Hurricane Sandy along the Atlantic Coast of the United States, October 2012. U.S. Geological Survey Open-File Report 2013–1043, 42 pp. https://doi.org/10.3133/ofr20131043

Meinen CS, Baringer MO, Garcia RF (2010) Florida Current transport variability: an analysis of annual and longer-period signals. Deep-Sea Res 57(7):835–846. https://doi.org/10.1016/j.dsr.2010.04.001

Oey LY, Ezer T, Wang DP, Fan SJ, Yin XQ (2006) Loop Current warming by Hurricane Wilma. Geophys Res Lett 33:L08613. https://doi.org/10.1029/2006GL025873

Oey LY, Ezer T, Wang DP, Yin XQ, Fan SJ (2007) Hurricane-induced motions and interaction with ocean currents. Cont Shelf Res 27: 1249–1263. https://doi.org/10.1016/j.csr.2007.01.008

Park J, Sweet W (2015) Accelerated sea level rise and Florida current transport. Ocean Sci 11:607–615. https://doi.org/10.5194/os-11-607-2015

Piecuch CG, Ponte RM (2015) Inverted barometer contributions to recent sea level changes along the northeast coast of North America. Geophys Res Lett 42:5918–5925. https://doi.org/10.1002/2015GL064580

Piecuch CG, Dangendorf S, Ponte R, Marcos M (2016) Annual sea level changes on the North American Northeast Coast: influence of local winds and barotropic motions. J Clim 29:4801–4816. https://doi.org/10.1175/JCLI-D-16-0048.1

Sallenger AH, Doran KS, Howd P (2012) Hotspot of accelerated sea-level rise on the Atlantic coast of North America. Nat Clim Chang 2:884–888. https://doi.org/10.1038/NCILMATE1597

Shay LK, Goni GJ, Black PG (2000) Effects of a warm oceanic feature on hurricane Opal. Mon Weather Rev 128:1366–1383. https://doi.org/10.1175/1520-0493(2000)128<1366:EOAWOF>2.0.CO;2

Tallapragada V, Bernardet L, Biswas MK, Gopalakrishnan S, Kwon Y, Liu Q, Marchok T, Sheinin D, Tong M, Trahan S, Tuleya R, Yablonsky R, Zhang X (2014) Hurricane Weather Research and Forecasting (HWRF) Model: 2014 Scientific Documentation. Editor: L. Bernardet. NCAR Development Tested Bed Center Report, 81pp, Boulder, CO.

Todd RE, Asher TG, Heiderich J, Bane JM, Luettich RA (2018) Transient response of the Gulf Stream to multiple hurricanes in 2017. Geophys Res Lett 45:10,509–10,519. https://doi.org/10.1029/2018GL079180

Wdowinski S, Bray R, Kirtman BP, Wu Z (2016) Increasing flooding hazard in coastal communities due to rising sea level: case study of Miami Beach, Florida. Ocean Coast Manag 126:1–8. https://doi.org/10.1016/j.ocecoaman.2016.03.002

Wu CR, Chang YL, Oey LY, Chang CWJ, Hsin YC (2008) Air-sea interaction between tropical cyclone Nari and Kuroshio. Geophys Res Lett 31:L12605. https://doi.org/10.1029/2008GL033942

Yablonsky RM, Ginis I, Thomas B, Tallapragada V, Sheinin D, Bernardet L (2015) Description and analysis of the ocean component of NOAA's operational Hurricane Weather Research and Forecasting (HWRF) Model. J Atmos Ocean Technol 32:144–163. https://doi.org/10.1175/JTECH-D-14-00063.1